

INFLUENCE OF PRESSING AND DRYING ON THE MICROSTRUCTURE OF RECYCLED PLANT FIBERS

JINQUAN WAN, YAN WANG, YONGWEN MA and QING XIAO

*College of Environmental Science and Engineering, South China University of Technology,
Guangzhou, China, 510640*

Received October 21, 2008

The influence of pressing and drying on the microstructure of wheat straw fiber during reuse processes was studied. The results showed that, at an applied pressure below 4 MPa, the WRV loss rate was of 7.96%, while, at pressures over 4MPa, it was of 25.90%. When pressure increased from 1MPa to 5 MPa, cellulose crystallinity increased also, and the fiber cell wall pores closed to a great extent. With increasing pressure from 1 to 5 times, WRV decreased. However, cellulose crystallinity increased with increasing the number of pressings. Fiber pores were irreversibly and significantly closed after the first pressing while, with an increasing number of pressings, the changes observed in pore size and distribution of fibers were insignificant. When the drying temperature increased from 60 to 120 °C, cellulose crystallinity increased to 84.6% and the average pore volume corresponding to the mesopore decreased by $5.42 \times 10^{-5} \text{ cm}^3/\text{g}$. In addition, WRV decreased, cellulose crystallinity increased and the degree of non-reversible closure was enhanced, when increasing the drying time at 100 °C. Electronic microscope photographs evidence no non-restorable collapse deformation and folds on the fiber cell wall after pressing and drying, which modified the sizes and shapes of the fiber cell wall.

Keywords: pressing, drying, cellulose crystallinity, pore structure, recycled fiber

INTRODUCTION

The importance of recycled plant fibers as a raw material in paper production is constantly increasing.¹ In spite of their economic value, recycled fibers have long been known to have inferior strength properties as compared to virgin fibers. The effect of recycling on pulp properties depends on the unit operations included in the cycle. Generally, it is agreed that pulp properties deteriorate during recycling. Deterioration of the paper-making properties of recycled fibers is mainly due to the irreversible structural changes induced in the fiber wall by pulping, refining, pressing and drying processes.²⁻⁴ During a reuse cycle, fibers lose their conformability and swelling capacity, which is associated with the changing microstructure of the recycled fiber.^{5,6} Generally, a recycled fiber can not be reused after 3-5 recycling operations,

because its quality decays. From a scientific viewpoint, decay in the quality of recycled plant fibers is inevitable. Thus, one of the most challenging ideas is to understand as thoroughly as possible the mechanism of fiber decay during recycling.

During the last two decades, numerous studies devoted to the decay of recycled plant fiber during recycling processes have shown that, upon recycling, the strength properties of both fibers and paper are reduced. The researchers used mainly hornification to reflect the decay of recycled plant fiber and estimated⁷⁻¹¹ the decay degree by macroscopic evaluation indexes and physical performance of paper, such as the Water Retention Value (WRV). Such studies may contribute to further elucidating the decay mechanism of fiber during reuse processes, although they do not provide

thorough theoretical explanations on the fiber decay mechanism. Cellulose crystallinity and pore structure of the fiber cell walls are two important parameters that may affect the fiber properties. Inter-fiber bond strength is affected by crystallinity, while the porous structure of the fiber affects its polymerization ability, swelling and paper strength.¹¹⁻¹⁴ The WRV of the fiber, the cellulose crystallinity and porous structure of the fiber wall undergo some irreversible variation, if the drying and pressing conditions change during fiber recycling, which results in lower fiber strength and thus – in fiber decay. That is why, the study on the modification mechanism of the pore structure of the fiber cell wall and that of crystallinity, under different drying and pressing conditions, is especially important, but so far little research reports are available.

The changes produced in the pore structure of the fiber cell wall and in cellulose crystallinity were studied. The influence of different pressing pressure, pressing times, drying temperature and drying time values on the changes observed in the microstructure of recycled plant fibers was evaluated. The important practical implications of this analysis refer to the possible improvement in the strength properties of the recycled plant fiber, through the elucidation of the decay mechanism of the recycled plant fiber, under different drying and pressing conditions.

MATERIALS AND METHOD

Materials and sample preparation

The fiber used in the experiment was laboratory self-made soda-AQ wheat straw pulp. The handsheets were prepared on a British handsheet machine, according to Tappi standards. The grade of unbleached wheat straw pulp paperboard was of 200 g/m². Pressing was carried out on the squeezer. For pressing tests, pressure – applied only once within 6 min – was set from 1 MPa to 5 MPa. For pressing times tests, the pulp was repeatedly pressed, from 1 to 5 times, at 4.5 MPa; each pressing process lasted for 6 min and was followed by drying on the dryer. For the drying test, the temperatures ranged between 60 and 120 °C, for 15 min, at time intervals of 10, 15 and 20 min at 100 °C.

WRV determination

The WRV value was determined by the

centrifugal method,¹⁵ on pulp or paper with a dry weight equivalent to 1.5 g. Centrifugation was carried out at 3000 rpm for 15 minutes. After centrifugation, the fiber mat was weighed in a pre-weighed weighting bottle, subsequently dried in a drying oven at 105 ± 2 °C for 24 h and then re-weighed. WRV was calculated with the following equation: $WRV = [(m_1 - m_2)/m_2] \times 100$, where m_1 is the weight of the wet pulp after centrifugation and m_2 is the weight of the dry pulp (in grams).

Determination of crystallinity by X-ray diffraction

The X-ray diffraction patterns of the fiber samples were recorded on a D/max-2550PC18 kW diffractometer. Diffraction used CuK α , at a pipe pressure of 40 kV, and tube current of 30 mA. The degree of crystallinity was determined¹⁶ from the ratio of integral intensity of the crystalline portions to the total intensity of the sample, over a range of $2\theta = 4^\circ$ to 40° . Paper pattern was directly pasted on a testing gripper by glue and a diffraction test was performed.

The relative crystallinity index:

$$RCI = \frac{I_{020} - I_{am}}{I_{020}} \times 100\%$$

Crystallinity:

$$\alpha = \frac{I_{020}}{I_{020} + I_{am}} \times 100\%$$

where I_{020} is the intensity of the 020 peak, when 2θ , approximately equaling 22.5° , represents the diffraction intensity of the crystallizing area, and I_{am} is the intensity between the 020 and the 110 peaks, when 2θ , approximately equal to 18° , represents the diffraction intensity of the fiber amorphous area.

Determination of the infrared crystallinity index

The crystallinity index was determined by infrared spectroscopy measured with a Nicolet Nexus Company FTIR. During sample preparation, the freeze-dried pulps were reduced to small pieces prior to mixing with potassium bromide and transformed into pellets for analysis. The crystallinity index was calculated¹⁷ from the relative intensities of the infrared bands ratios of 1372/2900 cm⁻¹:

$$N-O'KI = \frac{I_{1372}}{I_{2900}} \times 100\%$$

where I_{1372} represents the intensity (1372 cm⁻¹) of the band belonging to the CH bending vibration and I_{2900} is the intensity (2900 cm⁻¹) of the band belonging to CH and CH₂ bending vibrations.

Low-temperature nitrogen absorption

Fiber pore structure was analyzed with a pore

size distribution detector ASAP2010M (USA, Micromeritics) with N_2 gas, according to the Brunauer–Emmett–Teller (BET) equation at 77 K. The micropore volume of the samples was tested by the method of de Boer *et al.*¹⁸

Transmission electron microscope (TEM) sample preparation and topographic observations

The samples were fixed in 4% glutaraldehyde made up in 0.1 M phosphate buffer (pH 7.2), postfixed in 1.0% osmium tetroxide, dehydrated in a progressive ethanol and acetone solution, embedded in Epon812, sectioned with LKS ultramicrotome and stained with uranyl acetate followed by lead citrate,¹⁹ then observed on a JEM-1010 transmission electron microscope and photographed.

RESULTS AND DISCUSSION

Effect of pressing on the microstructure of wheat straw fiber

Effect of pressure on cellulose crystallinity and porous structure

Figure 1 shows the effects of the applied pressure on both WRV and crystallinity, where α represents the cellulose crystallinity by X-ray diffraction. When pressure was below 4 MPa, the loss rate of WRV was of only 7.96%. However, WRV decreased

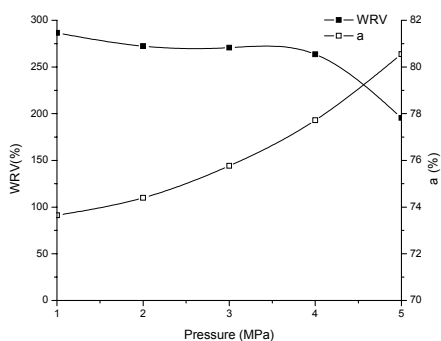


Figure 1: Effect of pressure on fiber WRV and cellulose crystallinity

Figure 2 also shows that the peaks of the fiber distribution curves ranged between 1.5 and 3 nm. After pressing at pressures of 1, 2, 3, 4, 5 MPa, the moisture content of the pulps was of 9.54, 8.74, 8.54, 7.72 and 6.18%, respectively. The results obtained show that the micropores were found predominantly in the fiber, together with numerous mesopores, while the macropores

obviously at a loss rate of 25.90%, when pressure exceeded 4 MPa. The reason was that the fiber became much more compact and the cell wall was seriously dehydrated under high pressure, which resulted in an irreversible loss in the swelling ability of the fiber. Also, crystallinity increased with increasing pressure.

Dubinin²⁰ divided the pores of porous solids into three groups: micropore (radius < 2.0 nm), mesopore (radius: 2~50 nm) and macropore (radius > 50 nm). Figure 2, illustrating the effects of pressure on fiber pore size distribution, shows that, after drying, the pore size was mainly distributed between 1.5 and 300 nm. However, no micropores were present in the raw pulp fiber. As to the pore structure of the raw fiber and that of the fiber treated at different pressures, mention should be made of an extended, irreversible closure of fiber mesopores, while the pore volume corresponding to mesopores was about 6 times lower in the treated pulp than in the raw pulp fiber. However, the macropores of all kinds of fiber showed no obvious change, permitting the deduction that they appeared after pressing, as derived from a part of the mesopores.

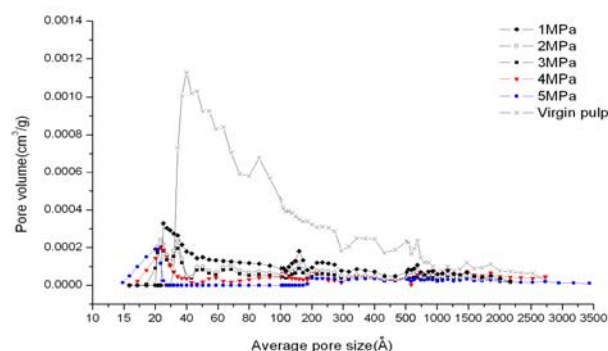


Figure 2: Effect of pressure on the fiber pore size distribution

were almost absent. When pressure reaches a value of 3 MPa, the curve evidences double peaks, ranging mainly from 1.5 to 4 nm. However, at 4 MPa, the curve presents only one peak. Compared to the curve recorded under 3 MPa, the pore volume corresponding to mesopores decreased and complete closure occurred in partial pores between 30 and 70 nm. When pressure increased to 5

MPa, complete closure occurred in partial pores between 2 and 20 nm, while the distribution of micropores and macropores was only slightly modified.

Figures 1 and 2 indicate that fiber crystallinity increased with increasing pressure, which might be caused by the fact that a high pressure enhanced the intermolecular hydrogen bonds of cellulose. With increasing pressure, the irreversible pore closure increased, and even complete closure occurred in partial pores.

Effect of pressing times on cellulose crystallinity and porous structure

Figure 3 shows the effects of pressing times on both WRV and fiber crystallinity, under the same pressure (4.5 MPa), applied for 6 min for each pressing process. It can be seen that, with an increasing number of pressings, WRV obviously decreased, while cellulose crystallinity increased.

Figure 4 plots the effects of different numbers of pressings on the fiber pore size and distribution. The moisture content of

virgin pulp and that of the pulps submitted to 1 to 5 pressings was of 25.64, 10.68, 9.98, 9.53, 9.26 and 9.16%, respectively.

It can be observed that the mean diameter of the fiber pores was of about 1.5~300 nm, most of the curve peaks being recorded between 1.5 and 2 nm, which permits the deduction that the micropores represent the main part of the fiber pores, some mesopores and macropores being also present. As compared to raw pulp, after pressing, the fiber pores were irreversibly closed to a great extent, while partial micropores and partial pores (between 2~10 nm) were completely closed. When increasing the number of pressings, the pore volume corresponding to micropores obviously increased. The changes in fiber pore size and distribution were not significant, comparatively with those in the fibers submitted to one, three and five pressings. The results indicate that the unbleached straw fiber pores were seriously and irreversibly closed after the first pressing, while the partial pores were completely closed, which affected fiber quality.

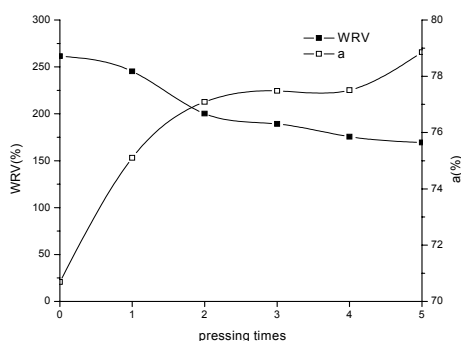


Figure 3: Effect of pressing times on fiber WRV and cellulose crystallinity

Effect of drying on the microstructure of wheat straw fibers

Effect of drying temperature on cellulose crystallinity and porous structure

Figure 5, showing the effects of drying temperature on both WRV and cellulose crystallinity, evidences that, with increasing drying temperature, WRV decreased, while crystallinity increased. When the drying temperature exceeded 100 °C, its influence on WRV and cellulose crystallinity was even higher.

Figure 6 illustrates the relationship

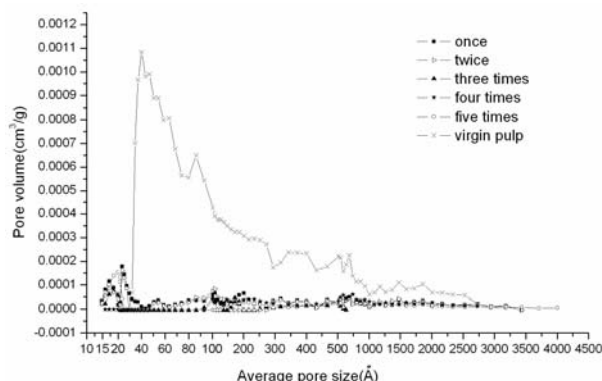


Figure 4: Pore size distribution of unbleached straw fiber at different pressing times

between the fiber pore sizes and pore size distribution at different temperatures. At drying temperatures of 80, 100 and 120 °C, the moisture content of both virgin pulp and treated pulps was of 25.64, 11.13, 10.82 and 10.48%, respectively.

Figure 6 shows that, after drying, the pore size was mainly distributed between 2 and 300 nm. When the drying temperature was above 100 °C, some micropores, smaller than 2.0 nm, were seen. Pore size decreased with increasing the drying temperature, the pore volume peaks being all between 2 and 5 nm.

Temperature had a notable effect on fiber mesopores, especially between 2 and 10 nm. As the drying temperature increased from 80 to 100 °C and from 100 to 120 °C, respectively, the average pore volume corresponding to mesopores decreased with $3.22 \times 10^{-5} \text{ cm}^3/\text{g}$ and $5.42 \times 10^{-5} \text{ cm}^3/\text{g}$, respectively. The results show that mesopores were found predominantly in the fiber, along with some macropores while, after drying, the micropores were almost absent. With increasing temperature, the pore volume corresponding to mesopores obviously decreased. The effect of the drying temperature on the fiber pore was mainly located in the mesopores.

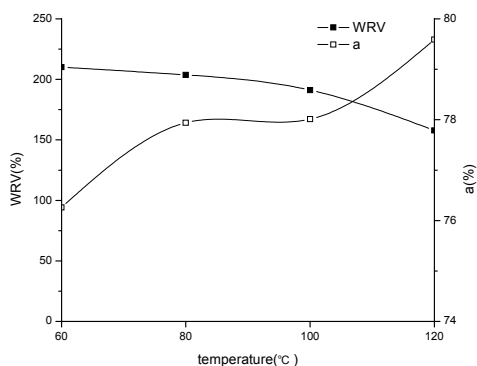


Figure 5: Effect of drying temperature on fiber WRV and cellulose crystallinity

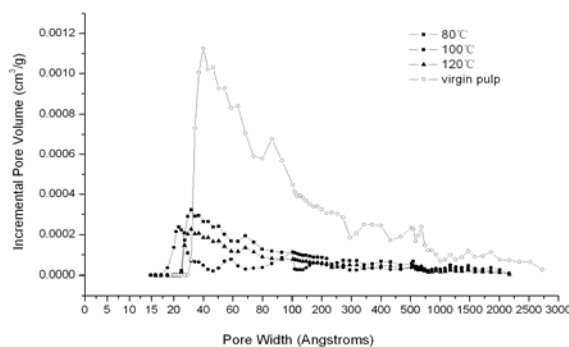


Figure 6: Effect of drying temperature on fiber pore size distribution

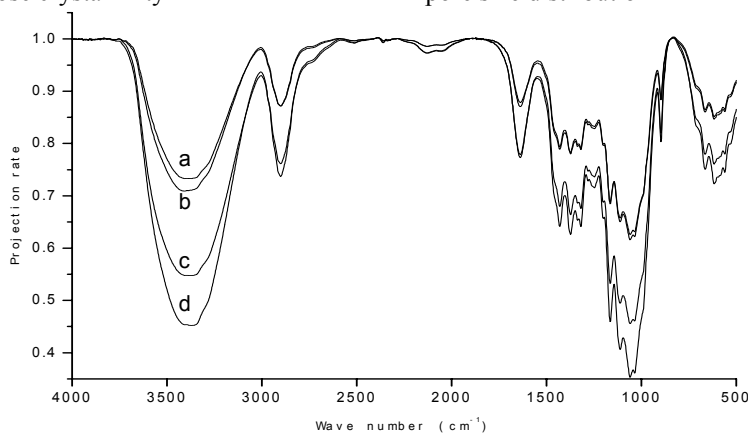


Figure 7: FTIR spectra of the samples dried at different temperature values:
a . 60 °C ; b. 80 °C ; c. 100 °C ; d.120 °C

Table 1
Effect of drying temperature on fiber N-O'KI and RCI

Drying temperature, °C	60	80	100	120
N-O'KI (%)	85.17	87.38	89.62	89.93
RCI (%)	68.87	71.70	72.07	74.36

According to Table 1, the value of N-O'KI and RCI increases with increasing the drying temperature. Figure 7, plotting the Fourier transform infrared (FTIR) spectra of cellulose at different temperatures, evidences peaks between 2800~3600 cm^{-1} at different drying temperatures, while, above 3200 cm^{-1} , the stretching vibration absorption peak of OH was evident. The width of the peak above 3200 cm^{-1} increased with increasing temperature, which indicated that the intramolecular hydrogen bondings were obviously enhanced after the increase in the drying temperature. Table 1 and Figure 7 show that cellulose crystallinity increased with increasing temperature, which might be caused by the enhancement of the intramolecular hydrogen bonding.

Effect of drying time on cellulose crystallinity and porous structure

The changes of WRV, cellulose crystallinity and porous structure of fiber under different drying time values were studied at a constant fiber drying temperature of 100 °C. Figure 8 shows the effects of the

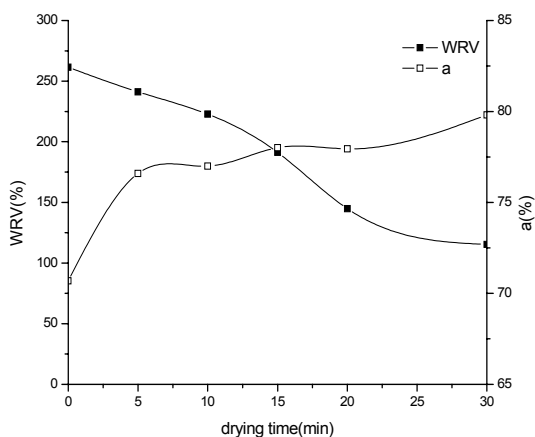


Figure 8: Effect of drying time on fiber WRV and cellulose crystallinity

Also, the average pore volumes corresponding to mesopores and micropores were both higher at a drying time of 10 min than at 15 min, which permits the conclusion that the degree of non-reversible closure was enhanced with increasing the drying time. The possible reason for this is that higher temperatures can promote a change from elastic to plastic deformation in the cell wall pore structure, which influences the

drying time on fiber WRV and cellulose crystallinity. The result indicates that the longer the drying time, the smaller the WRV, while fiber crystallinity increased gradually with the drying time. However, over a 5 min interval, crystallinity increased dramatically.

Figure 9 shows the effects of the drying time on fiber pore size and distribution, when the fiber drying temperature was maintained at 100 °C. The moisture content of virgin pulp was of 25.64%. After drying for 10, 15 and 20 min at 100 °C, the moisture contents were of 7.69, 6.36, 5.96%.

Figure 9 shows that some micropores appeared after a certain drying time. The pore volume peaks of the raw pulp fiber were between 2 and 6 nm, although, after different drying periods, they all were between 1.5 and 4 nm. Fiber pore volume decreased with increasing the drying time, which had a notable effect on the fiber mesopores, especially between 2 and 30 nm. In addition, the average pore volume corresponding to mesopores and micropores between 1.5 and 8 nm decreased to $4.15 \times 10^{-5} \text{ cm}^3/\text{g}$, at drying periods ranging from 10 to 15 min.

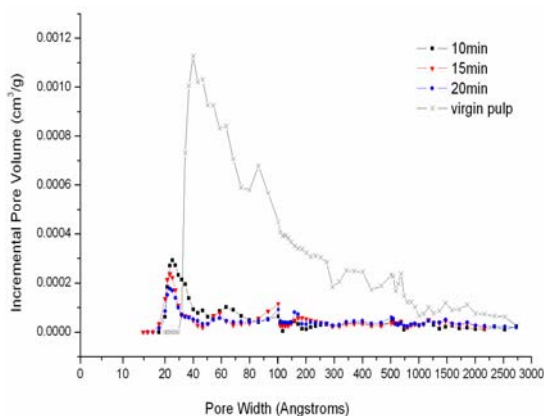


Figure 9: Effect of drying time on fiber pore size distribution

adsorption of free water in the fiber and has a reduced swelling capacity in water, resulting in a lower fiber quality.

Transmission electron microscopy analysis *Porous morphological structure of fiber cell wall*

Figure 10 plots the configuration of different parts of the straw fiber cell wall by TEM analysis.

Figure 10(a) evidences big and irregular shape flakes in the cell wall, which indicates average sizes of about 50 nm for the pores of the fiber cell wall. Long strip fiber pores in the middle of Figure 10(a) may be also observed, along with larger pores visible in the bending angles of Figure 10(b). Figure 10(c) illustrates the longitudinal section of the middle part of fiber, with larger pores in the straw fiber cell wall, most of them irregularly shaped. The results prove the occurrence of both mesopores and macropores in the straw fiber cell wall, their partial shape characteristic being visible. Figure 11 shows the magnified TEM picture of a fragment from the straw fiber cell wall.

Grain distribution on the cell wall was

reasonably homogeneous, yet with numerous fine flakes among the grains. It can be inferred that numerous micropores were present on the straw fiber cell wall. The results agreed with those obtained by nitrogen adsorption.

Straw fiber cell lumen and porous morphological structure

Figures 12 and 13 show the transverse section of the straw fiber and the magnified TEM picture of a fragment of single fibers after recycling.

Figure 12 evidences an obvious deformation and collapse of the cell lumen in unbleached straw fiber after rewetting, which was not restorable.

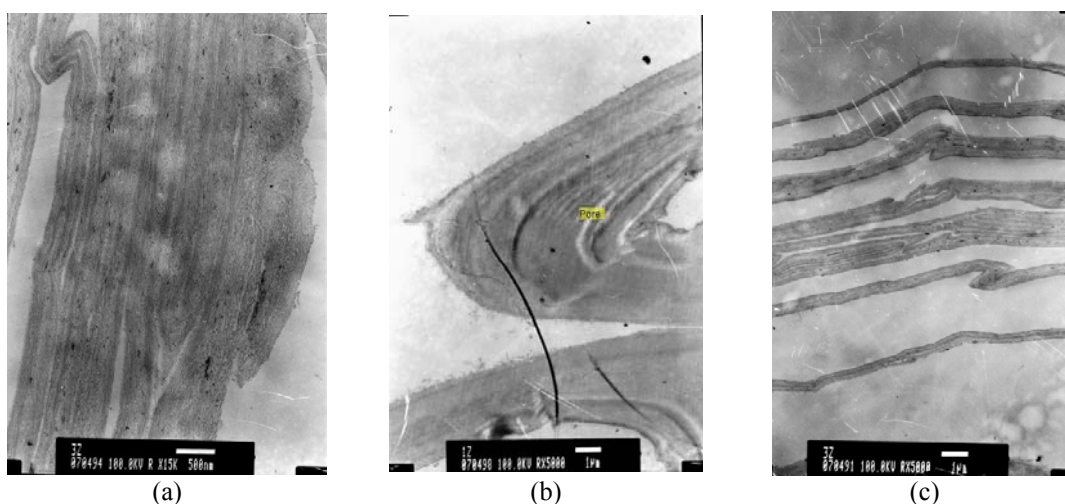


Figure 10: Configuration of different parts of the straw fiber cell wall: (a) TEM, size of image: $1 \times 1 \mu\text{m}$; (b) TEM, size of image: $1 \times 1 \mu\text{m}$; (c) TEM, size of image: $500 \times 500 \text{ nm}$

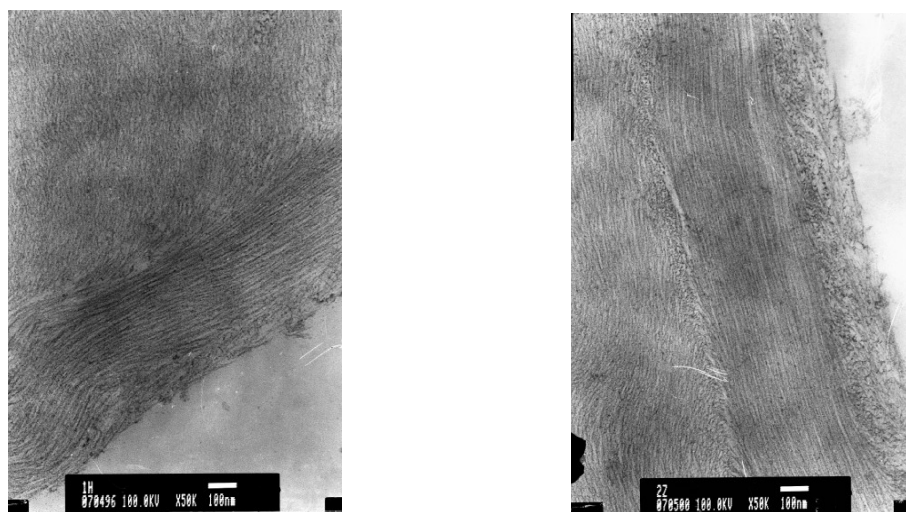


Figure 11: Magnified picture of a fragment of the straw fiber cell wall (TEM, size of image: $100 \times 100 \text{ nm}$)



Figure 12: Transverse section of straw fiber after one recycling (TEM, size of image: 2×2 μm)

The reason may be that, when the water filling the voids of the cell wall during papermaking treatments was evaporated, surface tension drew the cell wall together and the pore collapse closed larger voids, and also that the adhesion of the pore walls to each other resulted in the lamination of the cell wall lamellae. Cell wall collapse was not restorable. Even when the fibers contacted water once again, they did not swell completely.

The images show obvious folds on the cell wall of the straw fiber after dewatering by drying and pressing. It was deduced that these fold deformations made partial mesopores and macropores become smaller, thus causing the change in pore size, *i.e.* after one pressing and drying at 100 °C, the average pore volume corresponding to mesopores decreased with $3.22 \times 10^{-5} \text{ cm}^3/\text{g}$, as compared to the raw pulp fiber. Based on the fiber pore structure, Figure 13 shows that, after recycling, the straw fiber pores were irreversibly closed to a certain extent.

CONCLUSIONS

When the pressure applied was below 4 MPa, WRV was only slightly changed and the loss rate was of only 7.96%, increasing up to 25.90% at a pressure above 4 MPa. With increasing pressure, cellulose crystallinity increased and the fiber cell wall pore closed to a large degree. On the other hand, with an increasing number of pressings, WRV decreased, while cellulose crystallinity increased. The fiber pores were irreversibly



Figure 13: Part of single fiber after one recycling (TEM, size of image: 2×2 μm)

closed to a great extent after pressing, and even the partial pores were completely closed. However, with increasing the number of pressings, the changes observed in the fiber pore size and distribution were insignificant.

As the drying temperature increased from 60 to 120 °C, fiber crystallinity increased to 84.6% and the average pore volume corresponding to the mesopores decreased with $5.42 \times 10^{-5} \text{ cm}^3/\text{g}$. Meanwhile, WRV decreased, as well as the average pore volume corresponding to the mesopores, while cellulose crystallinity increased with increasing the drying time.

Electronic microscope images evidence non-restorable collapse deformation and folds on the fiber cell wall after pressing and drying, which changed the sizes and shapes of the fiber cell wall.

REFERENCES

- ¹ G. Jayme, *Wochenbl. Papierfabr.*, **6**, 187 (1944).
- ² R. L. Ellis and K. M. Sedlachek, in *Secondary Fiber Recycling*, Tappi Press, 1993, p. 7.
- ³ W. T. Tze and D. J. Gardner, *J. Adhes. Sci. Technol.*, **15**, 223 (2001).
- ⁴ U. Weise and H. Paulapuro, *JPPS*, **5**, 163 (1999).
- ⁵ O. Somwang, T. Enomae and F. Onabe, *Procs. 68th Pulp Paper Res. Conf.*, 2001, p. 16.
- ⁶ R. H. Newman, *Cellulose*, **11**, 45 (2004).
- ⁷ N. Wistara, *Cellulose*, **6**, 291 (1999).
- ⁸ A. Vainio and H. Paulapuro, *Nord. Pulp Pap. Res. J.*, **22**, 403 (2007).
- ⁹ B. Cao, U. Tschirner and S. Ramaswamy, *Tappi J.*, **81**, 119 (1998).

- ¹⁰ R. C. Howard, *J. Pulp Pap. Sci.*, **18**, 151 (1992).
- ¹¹ T. T. Maloney, T. Q. Li, U. Weise and H. Paulapuro, *Appita J.*, **50**, 301 (1997).
- ¹² M. Häggkvist, *Cellulose*, **5**, 33 (1998).
- ¹³ T. C. Maloney, *J. Pulp Pap. Sci.*, **25**, 12 (1999).
- ¹⁴ M. T. R. Bhuiyan, N. Hirai and N. Sobue, *J. Wood Sci.*, **46**, 431 (2000).
- ¹⁵ E. F. Thode, Jr., J. G. Bergomi and R. E. Unson, *Tappi J.*, **43**, 505 (1960).
- ¹⁶ M. T. R. Bhuiyan, N. Hirai and N. Sobue, *J. Wood Sci.*, **47**, 336 (2001).
- ¹⁷ S. Tasker, J. P. S. Badyal, S. C. E. Backson *et al.*, *Polymer*, **35**, 4717 (1994).
- ¹⁸ J. H. de Boer, B. G. Linsen and T. H. Von Der Plas, *J. Catal.*, **4**, 649 (1965).
- ¹⁹ H. Yoshiki, C. Bruno and S. Junji, *Cellulose*, **16**, 1 (2009).
- ²⁰ D. Topgaard, *Cellulose*, **9**, 139 (2002).